

Input shaping control of a nuclear power plant's fuel transport system

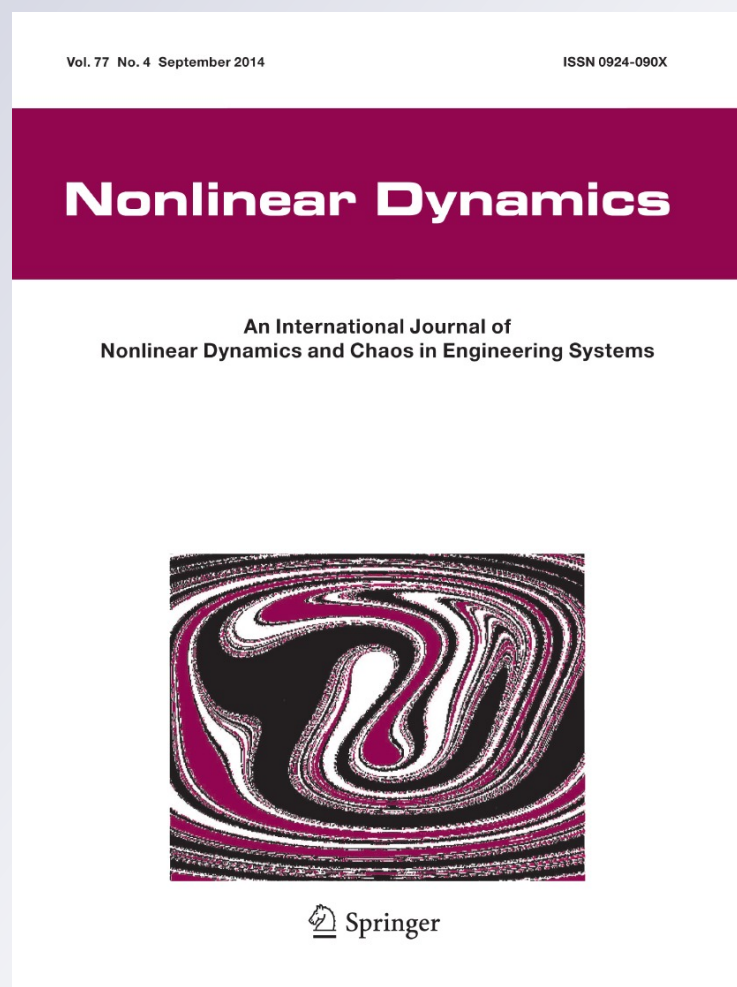
Umer Hameed Shah & Keum -Shik Hong

Nonlinear Dynamics

An International Journal of Nonlinear
Dynamics and Chaos in Engineering
Systems

ISSN 0924-090X
Volume 77
Number 4

Nonlinear Dyn (2014) 77:1737-1748
DOI 10.1007/s11071-014-1414-1



Your article is protected by copyright and all rights are held exclusively by Springer Science +Business Media Dordrecht. This e-offprint is for personal use only and shall not be self-archived in electronic repositories. If you wish to self-archive your article, please use the accepted manuscript version for posting on your own website. You may further deposit the accepted manuscript version in any repository, provided it is only made publicly available 12 months after official publication or later and provided acknowledgement is given to the original source of publication and a link is inserted to the published article on Springer's website. The link must be accompanied by the following text: "The final publication is available at link.springer.com".

Input shaping control of a nuclear power plant's fuel transport system

Umer Hameed Shah · Keum-Shik Hong

Received: 29 October 2013 / Accepted: 6 April 2014 / Published online: 23 April 2014
© Springer Science+Business Media Dordrecht 2014

Abstract In this paper, the residual vibration control problem of a nuclear power plant's fuel-transport system is discussed. The purpose of the system is to transport fuel rods to the target position within the minimum time. But according to observations, the rods oscillate at the end of the maneuver, causing an undesirable delay in the operation and affecting the system's performance in terms both of productivity and of safety. In the present study, a mathematical model of the system was developed to simulate the under-water sway response of the rod while keeping in view the effects of the hydrodynamic forces imposed by the surrounding water. Experiments were performed to validate the model's correctness. Further, simulation results were used to design the input shaping control that generates shaped velocity commands for transport of the fuel rods to the target position with the minimum residual vibration. It was observed that due to the under-water

maneuvering, the fuel-handling system behaves as a highly damped process and that the generated shaped velocity commands fail to effect the desired suppression of the residual vibration. Therefore, keeping in view the highly damped nature of the system, a modified shaped command was generated that transported the fuel rods to the target position with the minimum residual vibration.

Keywords Input shaping control · Residual vibration control · Nuclear power plant · Fuel-transport system

1 Introduction

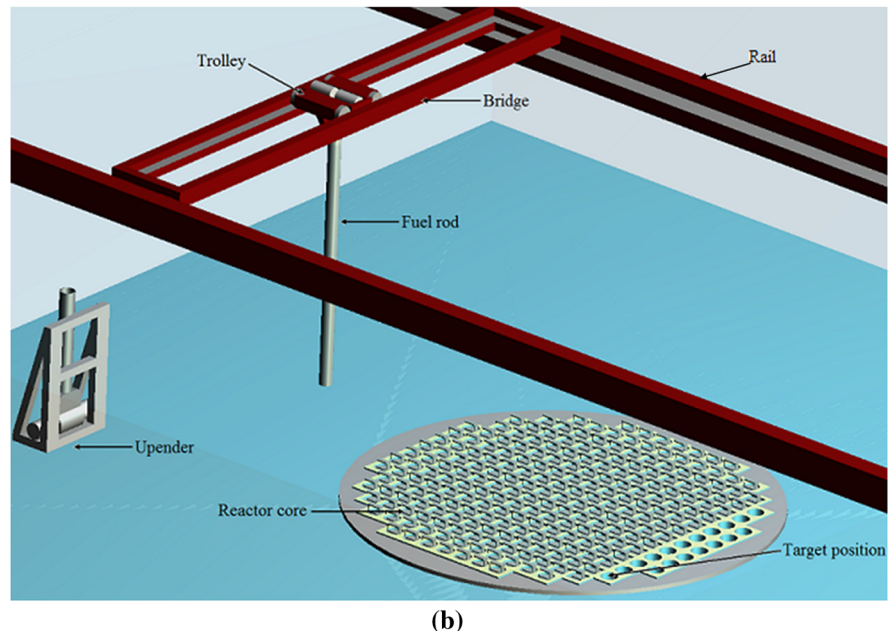
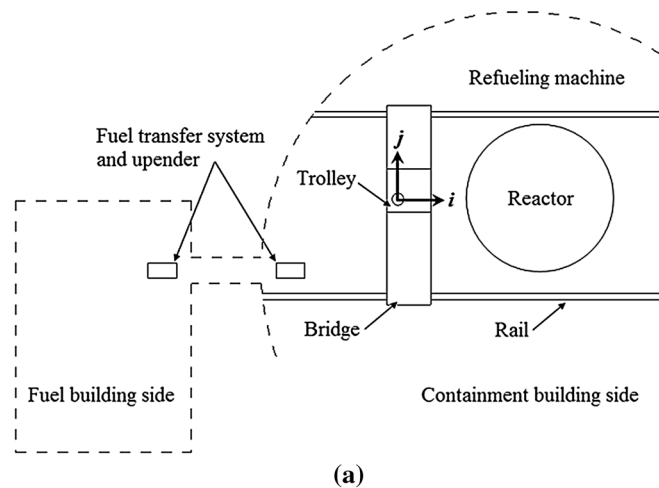
In this paper, the residual vibration control problem of a nuclear power plant's fuel-transport system (or fuel-handling system) is discussed. The system is required to transport fuel rods from given locations (i.e., reactor cores) to the target position (i.e., the fuel upender) and vice versa in the minimum time. The transportation of the fuel rods takes place under-water to prevent transference of their radiation to the environment. It has been observed, however, that the fuel rod starts to oscillate (i.e., manifest end-point oscillations) on reaching the target location, causing an undesirable delay in the operation and affecting the system's performance in terms both of productivity and of safety. The main research issue here is the fact that the considered objects are moved under-water, thus making for a highly damped system. It is expected that the load's

Electronic supplementary material The online version of this article (doi:[10.1007/s11071-014-1414-1](https://doi.org/10.1007/s11071-014-1414-1)) contains supplementary material, which is available to authorized users.

U. H. Shah
Department of Cogno-Mechatronics Engineering, Pusan National University, 2 Busandaehak-ro, Geumjeong-gu, Busan 609-735, Republic of Korea

K.-S. Hong (✉)
Department of Cogno-Mechatronics Engineering and School of Mechanical Engineering, Pusan National University, 2 Busandaehak-ro, Geumjeong-gu, Busan 609-735, Republic of Korea
e-mail: kshong@pusan.ac.kr

Fig. 1 Fuel-handling system in a nuclear power plant: **a** schematic of a fuel-handling system, **b** schematic of a refueling machine



oscillatory response in water would be quite different from that in air. Therefore, it is required first to investigate the under-water characteristics of the system by experimentation as well as simulation (i.e., theoretically) and then to design an appropriate control scheme for the suppression of residual fuel-rod vibrations in view of the hydrodynamic effects of the water.

A nuclear power plant generates electricity in a manner similar to that of a thermal power plant, the main difference being that the heat required for steam production is generated by the process of nuclear fission [1]. For this purpose, nuclear fuel rods are inserted into

nuclear cores located in a water pool. Continuous heat generation requires that spent fuel rods be replaced with fresh ones. Figure 1a depicts the new- and spent-fuel transporting process and its directionality between the reactor and the fuel building. Figure 1b illustrates the refueling machine (a type of over-head crane) and its transport of fuel rods between the reactor and the fuel-transfer system. Quick fuel-rod transference and placement are essential and require high positional accuracy.

Several control techniques are available for application to the suppression of residual vibrations [2–10]; they include adaptive control [2–4], open-loop control

[5], sliding-mode control [8], and fuzzy logic control [10]. However, because an over-head crane is used to transport and position fuel rods in a fuel-handling system, crane dynamics and control need to be considered [11, 12]. Unfortunately, feedback control in water is highly problematic, due to the difficulty of achieving functionality and integration of sensors in the fuel-handling system of a nuclear power plant [13]. In recent years, input shaping control (i.e., a type of feed-forward control) has been applied to address the vibration-suppression problem in oscillatory systems [14–20]. This is known to be the most feasible and practical control strategy for systems in which a pre-specified excitation is formulated and input to the system such that the system moves to the desired position without encountering residual vibration. Various versions of this technique include the zero-vibration (ZV) shaper [14], the zero-vibration derivative (ZVD) shaper [15], the extra-insensitive shaper [16, 17], and the specified intensity shaper [18, 19]. The technique is indeed versatile: it can be applied to a broad range of problems related to spacecraft, robotics, and MEMS [21–23].

Input shaping control has been widely applied to crane systems as well [24–29]. This notwithstanding, all of the previous relevant research has involved the moving of loads in air; moving them in water necessitates consideration of the effects of hydrodynamic forces on the system. Several studies have been carried on the effects of fluid-effected hydrodynamic forces on submerged objects [30–34], especially as pertain to water flow against a circular cylinder.

In the present study, a mathematical model for a fuel-handling system that transports objects in water was derived using the Lagrange equation. The hydrodynamic effects on the rod during its maneuver were incorporated into the model. Simulations and experiments were performed to validate the under-water responses of the developed model and the physical system, respectively. A bridge movement profile was shaped in such a way that, at the end of the bridge movement, the residual vibration of the fuel rod was minimized. It was observed that the shaped velocity profiles obtained by the ZV and ZVD controls of the crane working in the air did not work in our case. This is due to the fact that a sudden change of bridge velocity in air will bring a quick change of load in air, but not in water. Therefore, the input shaping technique in water needs to be modified in such a way that the shaped velocity profile increases (or decreases)

gradually from one velocity level to another, resulting in an improved under-water rod response. Experimental results confirmed that the modified shaped command profile successfully suppresses the residual vibration of the system considered.

The rest of the paper is structured as follows. Section 2 introduces the physical system and its response in view of the hydrodynamic forces acting on it along with the derived mathematical model. Section 3 discusses simulations and experiments that were performed on the system without any control. Section 4 presents the input shaping control formulation and its implementation. Finally, Sect. 5 analyzes the results for the input shaping control and draws conclusions.

2 Problem formulations

It is assumed that the fuel rod is a cylinder with a circular cross-section, that the water is at rest, and that the sway motions of the rod occur on the vertical plane consequent upon one-directional motions of the bridge or trolley. Figure 2 provides a schematic of the fuel-transport system studied in the experimentation, where $x(t)$ is the displacement of the bridge along the i -axis, M is the mass of the bridge, F_t is the force input along

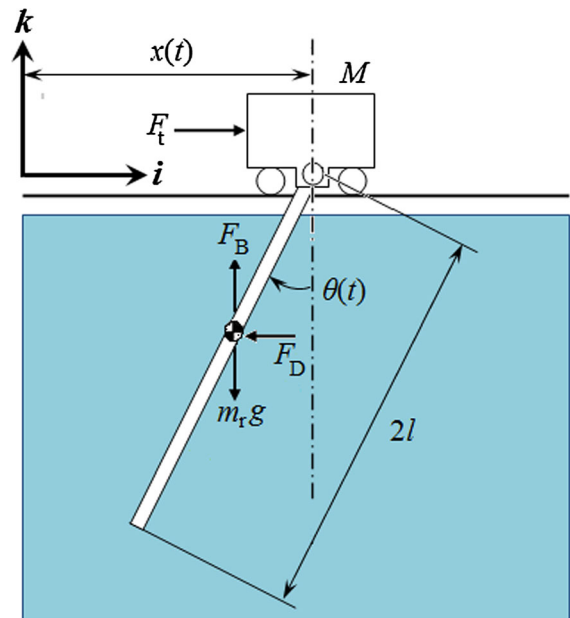


Fig. 2 Schematic of the fuel-transport system used in the experiment

the i -axis, l is the half-length of the rod, $\theta(t)$ is the sway angle of the rod, m_r is the rod mass, g is the gravitational acceleration, F_B is the buoyancy force, and F_D is the drag force (F_B and F_D being the hydrodynamic forces caused by the interaction of the maneuvered fuel rod with the surrounding fluid (water)).

2.1 Hydrodynamic forces

Whenever a body moves inside a fluid, there occurs a body-fluid interaction that can be described in terms of the hydrodynamic forces at the fluid-body interface. The hydrodynamic forces that act on the fuel rod during its under-water maneuver consist of the buoyancy force, the drag force, and the force due to added mass. The buoyancy force is the weight of the fluid displaced by the rod and is expressed mathematically as

$$F_B = \rho_w V_r g, \tag{1}$$

where ρ_w is the density of the fluid (water), and V_r is the volume of the submerged rod.

The drag force F_D is often termed the fluid reaction force that acts in the direction opposite to the rod's travel. Theoretically, the drag force F_D has two sources, the normal pressure and the skin friction [30], and is mathematically expressed in quadratic form as

$$F_D = \frac{1}{2} C_D \rho_w A_P |v_r| v_r, \tag{2}$$

where C_D is the drag coefficient, A_P is the projected frontal area, and v_r is the relative velocity between the fluid and the rod. In this paper, the drag coefficient given in [35],

$$C_D = \frac{5.93}{\sqrt{Re}} + 1.17 = 1.28, \tag{3}$$

where Re is the Reynolds number, is used. For the considered case, $Re = 2,946$ (the calculation is shown in Sect. 2.2, below). Whenever a submerged body accelerates in a fluid, the driving force must overcome not only the drag force but also the body's inertia and the inertia of any fluid accelerated by the body. The hydrodynamic force caused by acceleration of the fluid is called the added mass force F_a , and is expressed as

$$F_a = m_a \frac{dv_r}{dt}, \tag{4}$$

where m_a is the added mass, which is mathematically given as

$$m_a = C_a \rho_w V_r, \tag{5}$$

where C_a is the added mass coefficient. For the purposes of our system, the fuel rod is transported at a constant velocity; therefore, F_a is considered only for the oscillatory response of the rod. C_a is given in [30], for the case of a circular cylinder oscillating under-water at small amplitudes, as

$$C_a = 2 + \frac{4}{\sqrt{\pi\beta}} = 2.00, \tag{6}$$

where β is the frequency parameter, given as

$$\beta = \frac{fl^2}{\nu}, \tag{7}$$

where f is the oscillation frequency of the rod taken as 2.8 rad/s, l is the half-length of the rod, and ν is the kinematic viscosity of the water, given as 1.12×10^{-6} m²/s.

Several studies have been carried out to investigate the effects of the hydrodynamic forces caused by the flow across a submerged circular cylinder [30–33], revealing the important role of C_D and C_a in simulating the correct response of the submerged cylinder. McLain and Rock [32] have shown that the values of the hydrodynamic coefficients initially vary as the cylinder starts to accelerate in water, before attaining a constant value after the wake behind it is fully developed.

2.2 Under-water response

In order to estimate the Reynolds number at the maximum speed of the bridge, the problem of transporting the fuel rod under-water is compared with the case in which water flows against a circular cylinder, where the upstream velocity is constant both in time and location. Due to this fluid-structure interaction, the shear stresses and normal stresses are developed as a result of fluid viscosity and pressure, respectively. The flow across a circular cylinder varies with the Reynolds number, such that for $Re < 1$, the viscous effects are important,

and the streamlines about the center of the cylinder are symmetric. However, for larger Reynolds number, the flow-field region in which the viscous effects are important is very small; correspondingly, the viscous effects are transferred downstream, and the flow loses its symmetry, thus causing flow separation, which results in a turbulent wake region behind the cylinder [35]. For the considered case, the Reynolds number can be calculated using the relation

$$Re = \frac{\rho_w v d}{\mu_w} = 2,946, \tag{8}$$

where the water density ρ_w is 1,000 kg/m³, the upstream velocity of the water (i.e., the maximum bridge speed) v is assumed to be 0.33 m/s, the rod diameter d is 0.01 m, and the dynamic viscosity of the water μ_w is given as 1.12×10^{-3} Ns/m². In this case, the rod movement at the maximum speed of the bridge occurs in the stream of a moderate Reynolds number, which is within the $10^3 < Re < 10^5$ range [35]. Henceforth, there exists a turbulent wake region behind the fuel rod, resulting in a minimal viscosity effect on the generated drag force.

2.3 Equations of motion

Using Lagrange's method, a mathematical model for suppression of the residual vibration of the rod at the end of its transference is developed. Two variables from Fig. 2, $x(t)$ and $\theta(t)$, are considered to be the generalized coordinates (it is assumed that the bridge and the trolley do not move at the same time due to the safety issue in the nuclear power plant). The center of gravity (CG) of the rod is given by

$$x_c = x - l \sin \theta, \tag{9}$$

$$z_c = -l \cos \theta. \tag{10}$$

The kinetic energy (T) of the bridge and the rod and the potential energy (U) of the rod are given as

$$T = \frac{1}{2} (M\dot{x}^2 + m v_c^2 + I\dot{\theta}^2), \tag{11}$$

$$U = l(m_r g - F_B)(1 - \cos \theta), \tag{12}$$

where m is the sum of the rod mass (m_r) and the added mass (m_a), v_c is the velocity of the CG, and I is the inertia of the rod. Note that v_c^2 is given as

$$v_c^2 = \dot{x}^2 + l^2 \dot{\theta}^2 \cos^2 \theta - 2l\dot{x}\dot{\theta} \cos \theta + l^2 \dot{\theta}^2 \sin^2 \theta. \tag{13}$$

The dissipation energy (D) is given by

$$D = \frac{1}{2} (D_x \dot{x}^2 + D_\theta \dot{\theta}^2), \tag{14}$$

where D_x and D_θ correspond to the viscous damping coefficients associated with the movement of the bridge and the rod, respectively. The force input to the bridge and the drag force acting on the rod are the only generalized forces that exist for the considered system, thereby giving the generalized force

$$Q = \begin{bmatrix} F_t - F_D \\ 0 \end{bmatrix}. \tag{15}$$

Substituting (13), (14), and (15) into Lagrange's equation yields the equations of motion

$$(M + m)\ddot{x} - ml\ddot{\theta} \cos \theta + ml\dot{\theta}^2 \sin \theta + D_x \dot{x} + F_D = F_t, \tag{16}$$

$$ml\ddot{x} \cos \theta - \frac{7}{3}ml^2\ddot{\theta} - (m_r g - F_B)l \sin \theta + D_\theta \dot{\theta} = 0, \tag{17}$$

where F_B , F_D , and m_a are defined as in (1), (2), and (5), respectively. Assuming that $\cos \theta \approx 1$, $\sin \theta \approx \theta$, and $\dot{\theta}^2 \sin \theta \approx 0$ for small θ , the linear equations

$$(M + m_r + C_a \rho_w V_r)\ddot{x} - (m_r + C_a \rho_w V_r)l\ddot{\theta} + D_x \dot{x} + \frac{1}{2}C_D \rho_w A_P |v_r| v_r = F_t, \tag{18}$$

$$(m_r + C_a \rho_w V_r)l\ddot{x} - \frac{7}{3}(m_r + C_a \rho_w V_r)l^2\ddot{\theta} - g(m_r - \rho_w V_r)l\theta + D_\theta \dot{\theta} = 0 \tag{19}$$

are obtained. Solving (18) and (19) for theta-dynamics, the equation to be used for input shaping control,

$$\ddot{\theta} + C_1 \dot{\theta} + C_2 \theta = C_3(F_t - D_x \dot{x} - F_D), \tag{20}$$

is derived, where C_1 , C_2 and C_3 are given as

$$C_1 = \frac{-3(M + m_r + C_a \rho_w V_r)D_\theta}{(m_r + C_a \rho_w V_r)(7M + 4m_r + 4C_a \rho_w V_r)l^2},$$

$$C_2 = \frac{3g(M + m_r + C_a \rho_w V_r)(m_r - \rho_w V_r)}{(m_r + C_a \rho_w V_r)(7M + 4m_r + 4C_a \rho_w V_r)l},$$

$$C_3 = \frac{3}{(7M + 4m_r + 4C_a \rho_w V_r)l}.$$

Table 1 Simulation parameters

Parameters	Units	Value
Bridge mass (M)	Kg	5.1
Rod mass (m_r)	Kg	0.165
Half-length of the rod (l)	m	0.49
Rod diameter (d)	m	0.01
Drag coefficient (C_D)	–	1.28
Added mass coefficient (C_a)	–	2.00
Viscous damping coef. along the i -axis (D_x)	N-s/m	10.2
Viscous damping coef. along θ (D_θ)	Nm-s/rad	0.4



Fig. 3 Experimental setup

3 Simulation and experimentation

The under-water sway responses of the rod were simulated using the nonlinear model (16)–(17) and the parameters given in Table 1. Experimentation was then carried out to validate the mathematical model. Figure 3 shows the experimental setup used to study the under-water sway response of the system. Figure 4 compares the simulated responses using equations (16)–(17) with the experimental results: Fig. 4a shows the velocity profile of the bridge, according to which the maximum speed (0.33 m/s) was achieved in 0.25 s; Fig. 4b indicates that the target displacement (1.4 m) was achieved in 4.67 s; Fig. 4c compares the sway angles of the fuel rod. The values of D_x and D_θ are unknown;

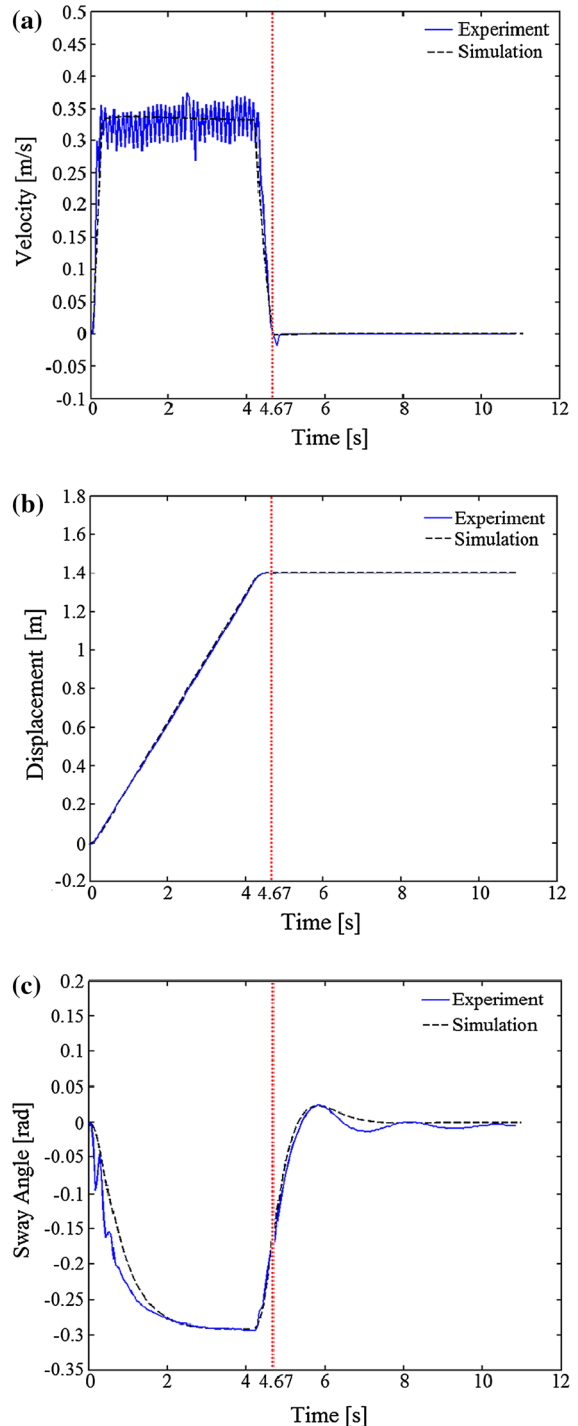


Fig. 4 Comparison of the under-water sway response of the rod for model verification. The simulation was carried out using Eqs. (16)–(17): **a** bridge velocity (unshaped), **b** bridge displacement, **c** sway angle of the rod

therefore, they were obtained by making the simulated sway response (the dotted line) to match the experimental result (the solid line). As can be seen in Fig. 4c, the simulated response matches the experimental result very closely, which reveals the validity of the developed mathematical model.

Further analyses of Fig. 4c reveal that the sway angle started to increase nonlinearly up to 0.29 rad during the initial 2.5 s period and stayed there for the remaining maximum-speed movement of the bridge. This was caused by the hydrodynamic forces discussed in Sects. 2.1–2.2 Also, the large sway angle of the rod was affected by the flow separation phenomenon behind the rod. It is noted, additionally, that the sway angle was not constant, until the wake was fully developed. It also is apparent that there was no oscillatory motion of the rod passing through the $-k$ -axis once the bridge began to maneuver (unlike the sway motion of a rod in air). This was due to the large damping provided by the hydrodynamic forces. However, once the bridge stops at its goal position, the rod will oscillate there. This is the phenomenon to be coped with using the mathematical model developed in Sect. 2. It may be noted that the simulated response at the start of the bridge maneuver did not exactly match with the actual response. The reason is that, in the simulation, C_D was assumed to be constant, whereas it actually changes continuously as a function of the wake formulation during these periods (see McLain and Rock [32]).

4 Control formulation and implementation

This section discusses the input shaping technique for the suppression of the residual vibrations of the considered system. As discussed earlier, input shaping can be used to generate different velocity/acceleration profiles for bridge travel that incurs the minimal residual vibration at the target position. Since it is our intention to transport the fuel rods to the target positions as quickly as possible, the trapezoidal velocity profile of the bridge speed is applied. Henceforth, in this section, the trapezoidal velocity profile shown in Fig. 4a will be convolved with impulses to generate the desired velocity profile of the bridge.

4.1 Mathematical model for input shaper design

In order to design the input shaper, the values of the system's natural frequency (ω_n) and the damping ratio

(ζ) are required for the oscillatory response of the rod (i.e., when the bridge has reached the target position). For the said case, the theta-dynamics given by (20) can be represented by the second-order system

$$\ddot{\theta} + 2\zeta\omega_n\dot{\theta} + \omega_n^2\theta = 0. \tag{21}$$

In order to obtain the values of ω_n and ζ for system (20), (21) was simulated using MATLAB. Then, they were adjusted to match the actual sway response of the rod as obtained from the experiment. The initial conditions, that is, the initial sway angle (θ_0) and the initial angular velocity ($\dot{\theta}_0$) of the rod, were obtained from the experimental data. As shown in Fig. 4, the bridge reached the target position in 4.67 s, and the corresponding sway angle of the rod at this instant was $\theta_0 = -0.17$ rad. The value for the angular velocity at 4.67 s ($\dot{\theta}_0$) was calculated as 0.22 rad/s. Figure 5 shows that the simulated response matched the experimental response for $\omega_n = 2.8$ rad/s and $\zeta = 0.56$.

These values of ω_n and ζ obtained by comparing the simulation with the experimental responses of the rod subsequently were used to design the ZV and ZVD shapers, as shown below. ZV Shaper:

$$\begin{bmatrix} A_i \\ t_i \end{bmatrix} = \begin{bmatrix} 0.9 & 0.1 \\ 0 & 1.35 \end{bmatrix}; \tag{22}$$

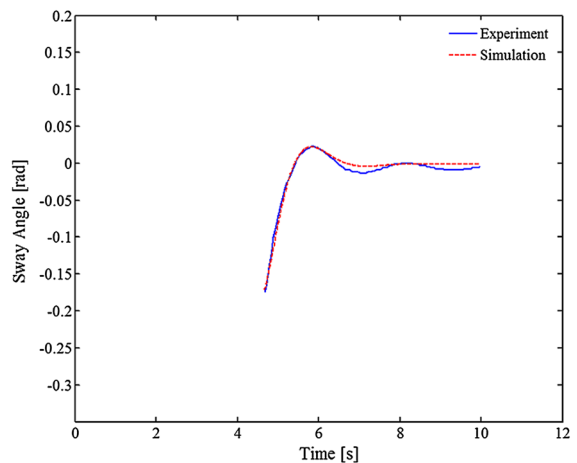


Fig. 5 Comparison of the experimental and simulated responses of the rod after the bridge stops at the target position. The simulation was carried out using Eq. (21) for $\omega_n = 2.8$ rad/s and $\zeta = 0.56$

ZVD Shaper:

$$\begin{bmatrix} A_i \\ t_i \end{bmatrix} = \begin{bmatrix} 0.8 & 0.18 & 0.02 \\ 0 & 1.35 & 2.7 \end{bmatrix} \quad (23)$$

where i corresponds to the number of impulses: the ZV shaper has two impulses, and the ZVD shaper has three impulses. A_i and t_i represent the magnitudes and the time locations, respectively, of the impulses of the given shaper.

4.2 Implementation of input shaper

The two input shapers in (22) and (23) were convolved with the unshaped velocity profile in Fig. 4a for the residual vibration suppression of the fuel rod. Figures 6 and 7 show the under-water sway responses of the fuel rod with the ZV and the ZVD shapers, respectively. Figures 6b and 7b show the two shaped velocity command profiles obtained by convolving the reference command with the ZV and the ZVD shaper, respectively. The shaped commands were used to drive the bridge, as shown in Figs. 6c and 7c, respectively, representing the bridge displacements for the given shaped commands. Figures 6d and 7d show the sway responses of the system for the two shaped command profiles. They indicate that the system responses obtained by the shaped velocity commands were not satisfactory, primarily because the convolution with the shaper caused sudden shifts in the shaped velocity profile, thereby effecting fluctuation in the sway response of the rod, as discussed earlier.

Therefore, in order to avoid the fluctuations in the sway response, it was required that a command profile without sudden shifts between the velocity steps be developed. For that purpose, the shaped command profile shown in Fig. 6b was altered in such a way as to remove all sudden shifts; in their places, gradual velocity shifts were introduced as constant deceleration steps between the velocity steps, which, as shown in Fig. 8, gained a significant improvement in the system's response. Figure 8b plots the modified shaped command, Fig. 8c the displacement of the bridge for the given command, and Fig. 8d the modified shaped command's improvement in the rod's sway response.

In this paper, we obtained the modified shaped command from the ZV shaper (shown in Fig. 6b) rather than

from the ZVD shaper (shown in Fig. 7b) for two reasons: the modification required the addition of deceleration between the velocity steps, and the last velocity step of the command obtained from the ZVD shaper was almost zero. Accordingly, the addition of deceleration between zero and the last velocity step does not affect the system's response, since the system is highly damped and does not respond to such small inputs; however, this will result in a prolonged command time.

5 Results and conclusions

Figure 8d shows the improved sway response of the rod as effected by the modified shaped command, compared with that of the rod without input shaping. The solid black line shows the experimental response of the rod for the modified shaped command, whereas the dashed red line and the dotted blue line show the simulation and experimental responses, respectively, without input shaping control. According to the figure, there was a significant drop in the overshoot of the sway response of the rod when the modified shaped command was used to drive the bridge: initially the sway angle reached the maximum value of 0.02 rad, but after applying the modified shaped command, the sway angle was reduced to a minor value of 0.003 rad, resulting in an approximate 85 % decrease in the maximum overshoot of the rod; moreover, the rod came to rest around 3 s earlier than the response generated by the unshaped command, thus resulting in a reduced settling time. These experimental results confirmed that the modified shaped profile generated by the input shaping technique successfully suppressed the residual vibration of the fuel-handling system.

In conclusion, this paper presents a mathematical model developed to simulate the response of a fuel rod transported by a nuclear power plant's fuel-handling system, considering the hydrodynamic forces acting on the fuel rod during its maneuver. Experimentation was conducted to validate the model and the selected hydrodynamic coefficients used in simulation. The simulated and experimental responses of the rod, showing the end-point oscillations, were used to design the ZV and the ZVD shapers by which the shaped velocity profiles were derived. These shaped velocity profiles, having been found ineffective for the considered case of under-water maneuvering, were therefore modified by adding

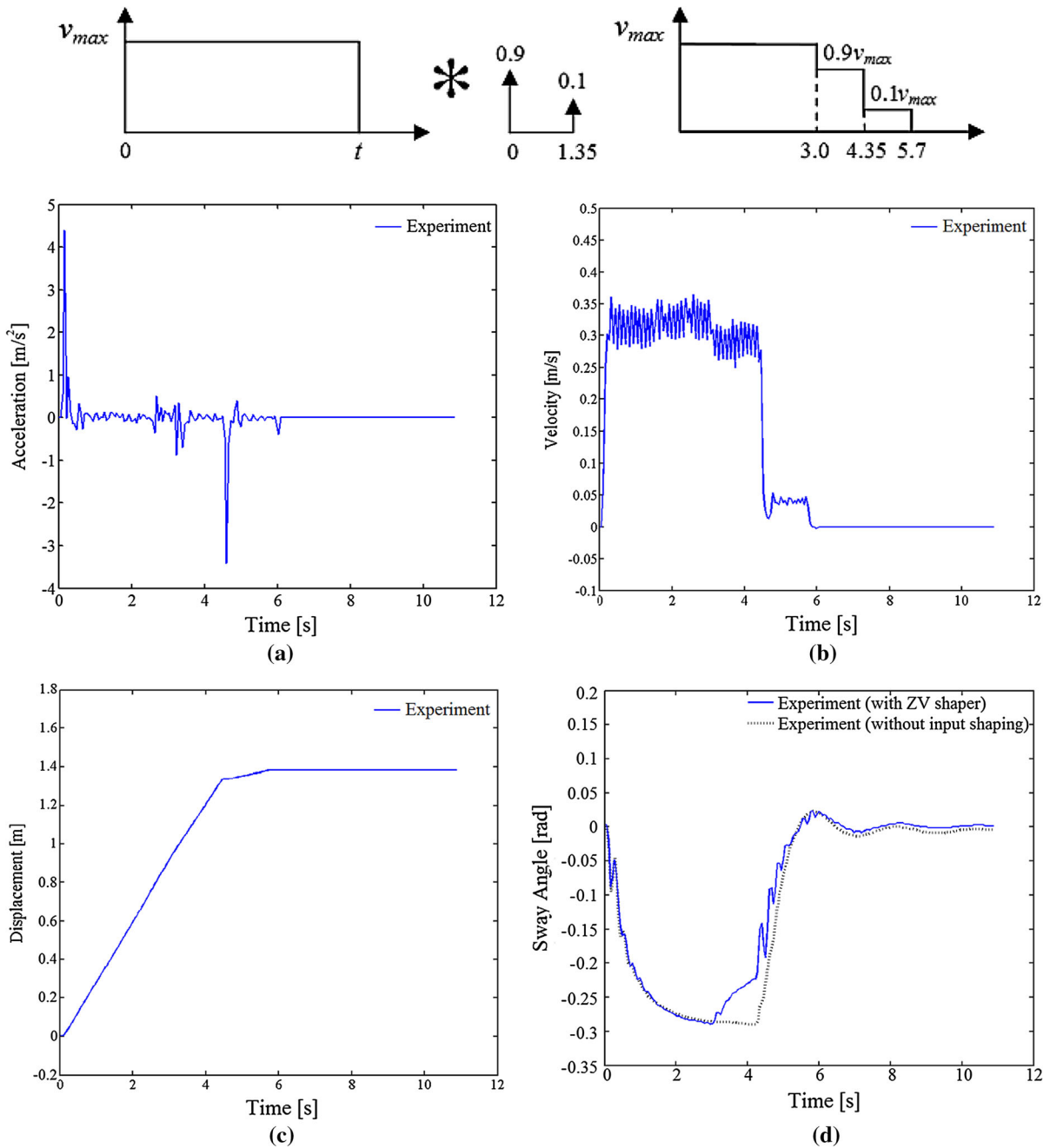


Fig. 6 Under-water sway response of rod with the ZV input shaper: **a** acceleration of the bridge for the ZV shaped velocity profile, **b** shaped velocity profile to drive the bridge obtained

from the ZV shaper, **c** position of the bridge for the ZV shaped velocity profile, **d** sway response of the rod for the ZV shaped velocity profile

deceleration between the velocity steps to minimize the fluctuations in the rod's sway response caused by those sudden velocity changes. This kind of input shap-

ing implementation to a fuel-transfer system entailing under-water oscillation had not, to our knowledge, been achieved prior to the present study. Previously, input

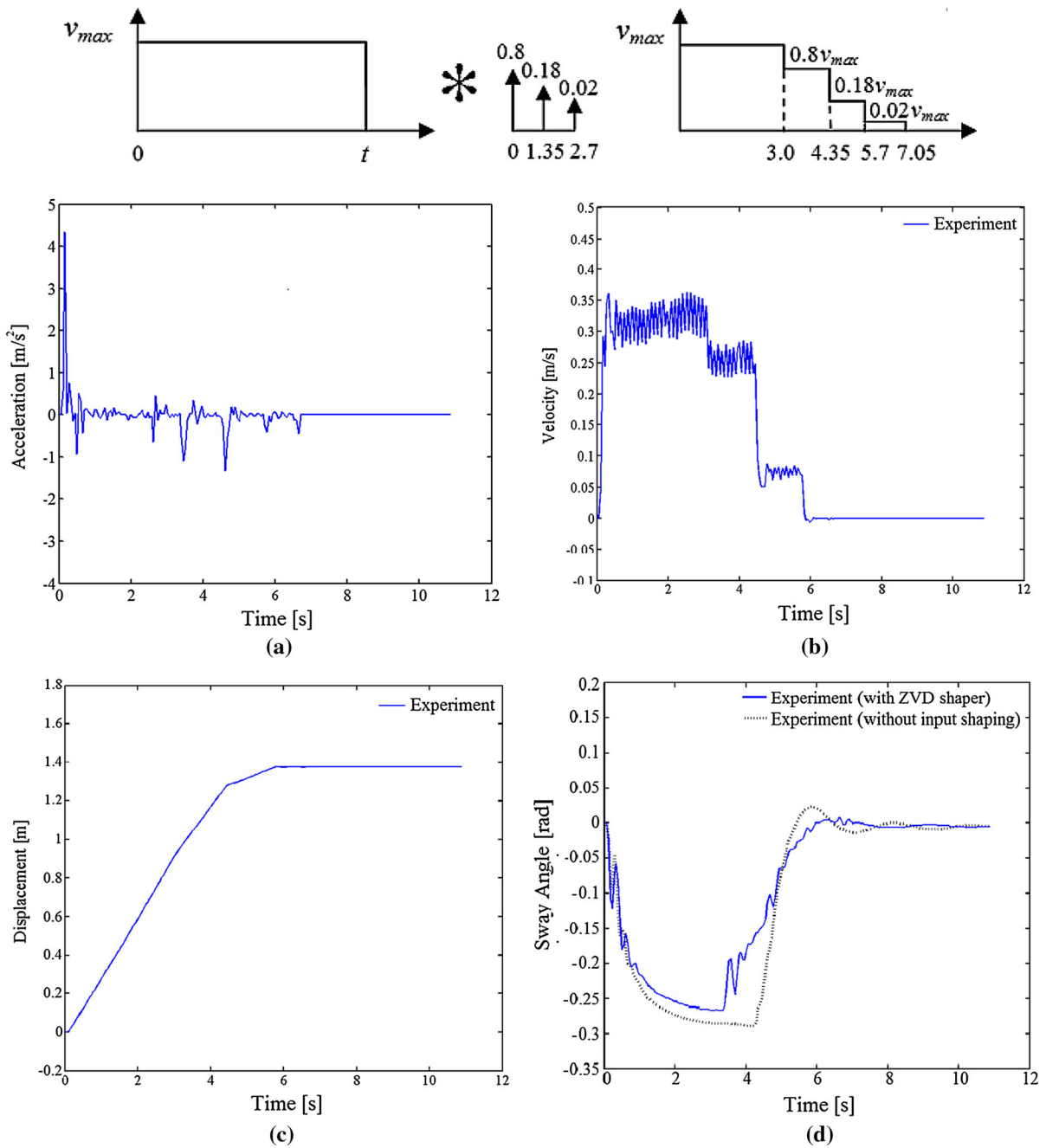


Fig. 7 Under-water sway response of rod with the ZVD input shaper: **a** acceleration of the bridge for the ZVD shaped velocity profile, **b** shaped velocity profile to drive the bridge obtained

from the ZVD shaper, **c** position of the bridge for the ZVD shaped velocity profile, **d** sway response of the rod for the ZVD shaped velocity profile

shaping had been applied only to un-damped systems like cranes. The present study, by contrast, using the modified input shaping technique, formulated a novel

approach to the suppression of residual vibration in a highly damped oscillatory system operating under-water.

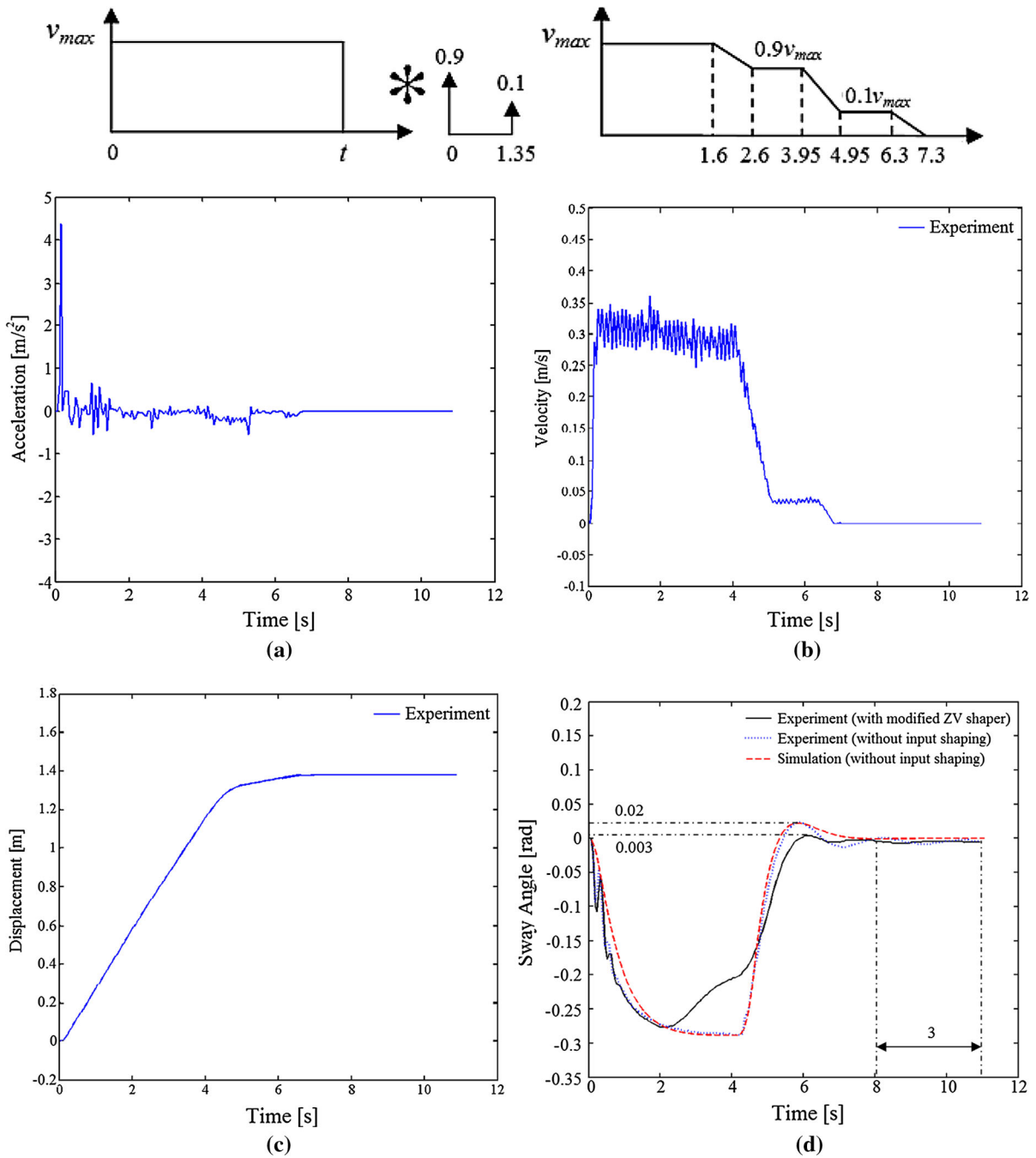


Fig. 8 Under-water sway response of rod for the modified shaped command: **a** acceleration of the bridge for the modified shaped command, **b** modified shaped command to drive the

bridge, **c** position of the bridge for the modified shaped command, **d** sway response of the rod with and without input shaping

Acknowledgments This research was supported by a grant from the Advanced Technology Center (ATC) Program funded by the Korean Ministry of Trade, Industry & Energy.

References

- Lee, S.S., Kim, S.H., Suh, K.Y.: The design features of the advanced power reactor 1400. *Nucl. Eng. Technol.* **41**(8), 995–1004 (2009)
- Hong, K.-S., Bentsman, J.: Direct adaptive control of parabolic systems: algorithm synthesis, and convergence and stability analysis. *IEEE Trans. Autom. Control* **39**(10), 2018–2033 (1994)
- He, W., Ge, S.S., How, B.V.E., Choo, Y.S., Hong, K.-S.: Robust adaptive boundary control of a flexible marine riser with vessel dynamics. *Automatica* **47**(4), 722–732 (2011)
- Ngo, Q.H., Hong, K.-S.: Adaptive sliding mode control of container cranes. *IET Control Theory Appl.* **6**(5), 662–668 (2012)
- Hong, K.-S.: An open-loop control for underactuated manipulators using oscillatory inputs: steering capability of an unactuated joint. *IEEE Trans. Control Syst. Technol.* **10**(3), 469–480 (2002)
- Rehan, M., Hong, K.-S.: Decoupled-architecture-based nonlinear anti-windup design for a class of nonlinear systems. *Nonlinear Dyn.* **73**(3), 1955–1967 (2013)
- El-Ganaini, W.A., Saeed, N.A., Eissa, M.: Positive position feedback (PPF) controller for suppression of nonlinear system vibration. *Nonlinear Dyn.* **72**(3), 517–537 (2013)
- Ngo, Q.H., Hong, K.-S.: Sliding-mode ant sway control of an offshore container crane. *IEEE/ASME Trans. Mechatron.* **7**(2), 201–209 (2012)
- He, W., Zhang, S., Ge, S.S.: Boundary control of a flexible riser with the application to marine installation. *IEEE Trans. Ind. Electron.* **60**(12), 5802–5810 (2013)
- Sagirli, A., Azeloglu, C.O., Guclu, R., Yazici, H.: Self-tuning fuzzy logic control of crane structures against earthquake induced vibration. *Nonlinear Dyn.* **64**(4), 375–384 (2011)
- Azeloglu, C.O., Sagirli, A., Edincliiler, A.: Mathematical modelling of the container cranes under seismic loading and proving by shake table. *Nonlinear Dyn.* **73**(1–2), 143–154 (2013)
- Abdel-Rahman, E.M., Nayfeh, A.H., Masoud, Z.N.: Dynamics and control of cranes: a review. *J. Vib. Control* **9**(7), 863–908 (2003)
- Fortgang, J., Singhose, W.: Concurrent design of vibration absorbers and input shapers. *J. Dyn. Syst. Meas. Control* **127**, 329–335 (2005)
- Smith, O.J.M.: *Feedback Control Systems*. McGraw-Hill, New York (1958)
- Singer, N.C.: Residual vibration reduction in computer controlled machines. Ph.D. thesis and MIT Artificial Intelligence Laboratory Technical Report No. 1030. Massachusetts Institute of Technology, Cambridge, MA (1990).
- Singer, N.C., Seering, W.P.: Preshaping command inputs to reduce system vibration. *J. Dyn. Syst. Meas. Control* **112**, 76–82 (1990)
- Singhose, W., Seering, W., Singer, N.: Residual vibration reduction using vector diagrams to generate shaped inputs. *J. Dyn. Syst. Meas. Control* **116**, 654–659 (1994)
- Park, U.H., Lee, J.W., Lim, B.D., Sung, Y.G.: Design and sensitivity analysis of an input shaping filter in the Z-plane. *J. Sound Vib.* **243**(1), 157–171 (2001)
- Singhose, W., Kim, D., Kenison, M.: Input shaping control of double pendulum bridge crane oscillations. *J. Dyn. Syst. Meas. Control* **130**(3), 034504 (2008)
- Singhose, W., Vaughan, J.: Reducing vibration by digital filtering and input shaping. *IEEE Trans. Control Syst. Technol.* **19**(6), 1410–1420 (2011)
- Singhose, W., Bohlke, K., Seering, W.: Fuel-efficient pulse command profiles for flexible spacecraft. *J. Guid. Control Dyn.* **19**(4), 954–960 (1996)
- Singhose, W.: Command shaping for flexible systems: a review of the first 50 years. *Int. J. Precis. Eng. Manuf.* **10**(4), 153–168 (2009)
- Daqaq, M.F., Reddy, C.K., Nayfeh, A.H.: Input-shaping control of nonlinear MEMS. *Nonlinear Dyn.* **54**(1–2), 167–179 (2008)
- Singhose, W., Porter, L., Kenison, M., Kriikku, E.: Effects of hoisting on the input shaping control of gantry cranes. *Control Eng. Pract.* **8**(10), 1159–1165 (2000)
- Hong, K.-S., Park, B.J., Lee, M.H.: Two-stage control for container cranes. *JSME Int. J. Ser. C* **43**(2), 273–282 (2000)
- Hong, K.T., Huh, C.D., Hong, K.-S.: Command shaping control for limiting the transient sway angle of crane systems. *Int. J. Control Autom. Syst.* **1**(1), 43–53 (2003)
- Blackburn, D., Singhose, W., Kitchen, J., Patrangenaru, P., Lawrence, J., Kamoi, T., Taura, A.: Command shaping for nonlinear crane dynamics. *J. Vib. Control* **16**(4), 477–501 (2010)
- Daqaq, M.F., Masoud, Z.N.: Nonlinear input-shaping controller for quay-side container cranes. *Nonlinear Dyn.* **45**(1–2), 149–170 (2006)
- Bhatta, D.D.: Computation of added mass and damping coefficients due to a heaving cylinder. *J. Appl. Math. Comput.* **23**(1–2), 127–140 (2007)
- Troesch, A.W., Kim, S.K.: Hydrodynamic forces acting on cylinders oscillating at small amplitudes. *J. Fluids Struct.* **5**(1), 113–126 (1991)
- Rahman, M., Bhatta, D.D.: Evaluation of added mass and damping coefficient of an oscillating circular cylinder. *Appl. Math. Model.* **17**(2), 70–79 (1993)
- McLain, T.W., Rock, S.M.: Development and experimental validation of an underwater manipulator hydrodynamic model. *Int. J. Robot. Res.* **17**(7), 748–759 (1998)
- Wang, L., Dai, H.L., Han, Y.Y.: Cross-flow-induced instability and nonlinear dynamics of cylinder arrays with consideration of initial axial load. *Nonlinear Dyn.* **67**(2), 1043–1051 (2012)
- Lin, C.-C., Chen, R.-R., Li, T.-L.: Experimental determination of the hydrodynamic coefficients of an underwater manipulator. *J. Robot. Syst.* **16**(6), 329–338 (1999)
- Munson, B.R., Young, D.F., Okiishi, T.H.: *Fundamentals of Fluid Mechanics*. Wiley, New York (2002)